

Photofission of ^{232}Th

J. D. T. Arruda-Neto, W. Rigolon, S. B. Herdade, and H. L. Riette

Instituto de Física, Universidade de São Paulo, São Paulo, Brazil

(Received 1 December 1983)

The bremsstrahlung-induced fission cross section of ^{232}Th was measured in the energy region of the giant dipole resonance. The data analysis, performed in terms of the bremsstrahlung spectrum calculated in the Davies-Bethe-Maximon approximation, shows that the photofission cross section measured at Livermore is more compatible with our results than the (γ, f) data from Saclay.

The characteristics of the fission decay of the isoscalar giant quadrupole resonance (GQR), namely, the branching ratios and strength distributions for actinide nuclei, have been studied by means of hadron- and electron-induced reactions. The results of these studies are controversial and somewhat obscure (Refs. 1 and 2, and references therein). The analysis of electron-induced reactions [inclusive electrofission (e, f) and coincident electrofission $(e, e'f)$] requires the precise knowledge of the related photofission cross sections $\sigma_{\gamma, f}$. For the (e, f) data analysis, $\sigma_{\gamma, f}$ is used to subtract the giant dipole resonance (GDR) contribution to the total electrofission yield.^{1,2} In the analysis of the $(e, e'f)$ data the photofission cross sections are necessary for the evaluation of the form factors at the "photon point."^{3,4} Therefore the photofission cross sections play a crucial role in the delineation of the GQR fission decay parameters.

Since the advent of monoenergetic photon beams, photoneutron cross sections have been measured systematically for most of the nuclides throughout the periodic table.⁵ Such investigations have been carried out particularly by the Livermore and Saclay laboratories. As a result of these efforts, the parameters of the GDR have been delineated; the neutron and fission branching ratios have been determined as well. However, careful examination of the Livermore and Saclay cross sections reveals serious discrepancies, especially regarding absolute values. The most alarming discrepancy is found in the photofission cross section $\sigma_{\gamma, f}$ of ^{232}Th , because the integrated cross section $A_{\gamma, f} = \int_0^{18} \sigma_{\gamma, f}(\omega) d\omega$ obtained at Livermore (ω is the excitation energy in MeV) is about 40% larger than the one obtained at Saclay, while the energy dependence of the $\sigma_{\gamma, f} \times \omega$ measured by these two laboratories is in good agreement.

This fact motivated us to perform a careful measurement of the bremsstrahlung-induced fission cross section for ^{232}Th . The main features of this experiment, when compared with earlier ones,⁵⁻⁷ are that (1) the intensity of the bremsstrahlung photon beam facilitates the measurement of fission yields with much better statistics; (2) the fission fragments are detected *directly* using mica foils track detectors, avoiding the need for a calculation of fission neutron multiplicity; and (3) the bremsstrahlung-induced fission cross section $\sigma_{B, f}$ is sensitive to the photofission area $A_{\gamma, f}$ (defined above), because

$$\sigma_{B, f}(E_e) = \int_0^{E_e} \sigma_{\gamma, f}(\omega) N^B(E_e, \omega) d\omega, \quad (1)$$

where E_e is the electron incident energy, and N^B is the bremsstrahlung spectrum. As N^B is to a reasonable approximation proportional to ω^{-1} we observe that² $\sigma_{B, f} \propto B(E1)P_f$, where $B(E1)$ is the reduced transition proba-

bility for the GDR, and P_f is the fission probability. Furthermore, $\omega_R B(E1)P_f \propto A_{\gamma, f}$, in the case that all of the GDR strength is concentrated in a single isolated level (the resonance peak) having an excitation energy ω_R .

We measured $\sigma_{B, f}(E_e)$, for E_e ranging from 20 to 32 MeV, using the electron beam of the University of São Paulo Linear Accelerator and mica foils as fission detector at different angles with respect to the incident beam direction. The absolute mass of the ^{232}Th target, $153 \mu\text{g}/\text{cm}^2$ thick, was determined by alpha counting to $\pm 4\%$. A copper radiator, $970 \text{ mg}/\text{cm}^2$ thick, was attached upstream of the target and the set was placed in the center of the reaction chamber making an angle of 45° with the electron beam. The electron beam was monitored by a secondary emission monitor (SEM), before the radiator and the target; calibration of the SEM to accuracy of $\pm 3\%$ was accomplished by comparison with a Faraday cup. The bremsstrahlung produced in the SEM aluminum foils contributed about 2% of the total bremsstrahlung-induced fission yield and this was corrected for. Contamination (of the order of 10%) of the photofission yields by electrofission events was accounted for by means of the method developed by Barber.⁸ The data were also corrected for the finite thickness of the radiator utilizing the procedures described in Ref. 9. This correction consists of dividing the radiator thickness into slices of $\sim 0.1 \text{ mg}/\text{cm}^2$ thick; the thin-target bremsstrahlung spectrum for each slice is calculated in the Davies-Bethe-Maximon approximation with Fermi-Thomas model screening functions,^{10,11} which is the most appropriate approach¹¹ in the energy region of the present experiment, taking into account the electron energy degradation in all the preceding slices. The evaluation of the integrated cross section $\sigma_{B, f}$ [Eq. (1)] is performed in a multiple-step process, for each $N^B(E_e, \omega)$ associated with a given slice of the radiator, using the routine SABRE2 available at this laboratory. Other details concerning the beam monitoring device, reaction chamber, accelerator, etc., were published elsewhere.^{2,9}

The fission fragments angular distributions were found to be isotropic. The solid angle of the fission detector is defined by the area of the mica foil and the radius of the reaction chamber (the distance from sample to detector). Figure 1 shows that results of this work for $\sigma_{B, f}$; the error bars (typically $\sim 7\%$) include both count-rate statistics ($\sim 1\%$) and systematic uncertainties (in the target thickness, detectors, solid angles, and beam monitoring device). The shaded bands were obtained by numerical integration of the photofission cross sections from Saclay and Livermore in the kernel of Eq. (1), using the procedure described above. Values of the $\sigma_{\gamma, f}$ cross section above 18 MeV were obtained by extrapolation of the experimental points below 18

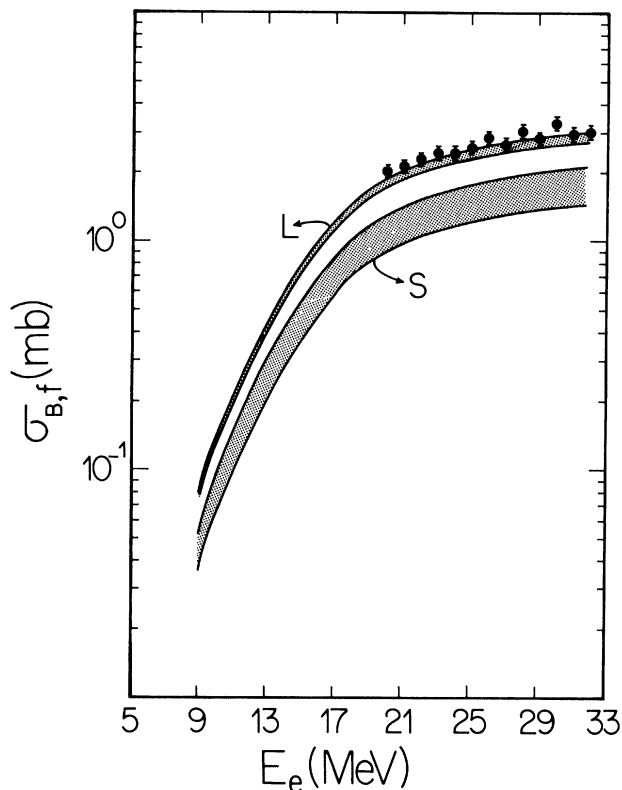


FIG. 1. Data points: bremsstrahlung-induced fission cross sections for ^{232}Th . Shaded bands: photofission cross sections from Saclay (S) and Livermore (L) integrated in the bremsstrahlung spectrum (details in the text); the width of the bands represents the experimental uncertainties associated with the photofission cross sections.

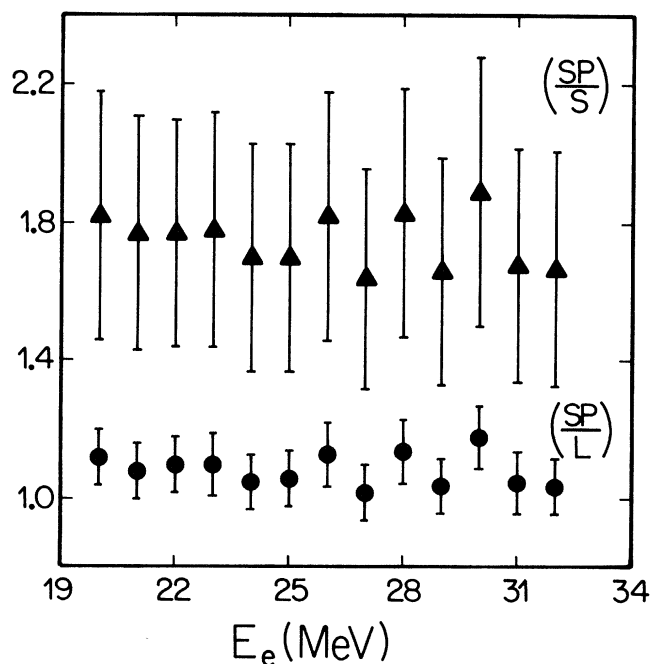


FIG. 2. Ratio of the bremsstrahlung-induced fission cross sections, from the present work (SP), to those generated from the Saclay (S) and Livermore (L) photofission cross sections.

MeV using a Lorentz curve. However, it should be noted that the integral cross sections $\sigma_{B,f}(E_e)$ for $E_e > 18$ MeV are nearly insensitive to small changes in the tail of the GDR till ~ 30 MeV. For instance, recalculating $\sigma_{B,f}$ with the assumption that $\sigma_{\gamma,f}$ is equal to zero for $\omega \geq 18.5$ MeV we found that for (a) $E_e = 20$ MeV, the cross section $\sigma_{B,f}$ decreases $\sim 1\%$, and for (b) $E_e = 30$ MeV, $\sigma_{B,f}$ decreases $\sim 8\%$ in comparison with the value shown in Fig. 1 (shaded band). Therefore the presence of structures (arising from fourth- and fifth-chances fission) sticking out from the smooth tail of the GDR will not affect the main conclusions of the present work. By the way, the third-chance fission barrier is ~ 17 MeV (Ref. 12) for ^{232}Th , while fourth- and fifth-chance should have fission barriers located at energies ≥ 22 MeV.

In Fig. 2 are shown the ratio of $\sigma_{B,f}$ measured in this laboratory to those calculated using the $\sigma_{\gamma,f}$ from the literature (see Fig. 1). In order to simplify the notation we name these ratios as SP/L and SP/S, standing for São Paulo/Livermore and São Paulo/Saclay, respectively. The mean values of the ratios (with the dispersion from the mean) are

$$\left\langle \frac{\text{SP}}{\text{L}} \right\rangle = 1.09 \pm 0.05, \quad \left\langle \frac{\text{SP}}{\text{S}} \right\rangle = 1.75 \pm 0.08.$$

Figure 3 demonstrates how the utilization of the available photofission data affects the interpretation of an electrofission experiment. In this figure the data points are ^{232}Th electrofission cross sections measured at Giessen.¹³ The curves in Fig. 3 were obtained by integrating the photofis-

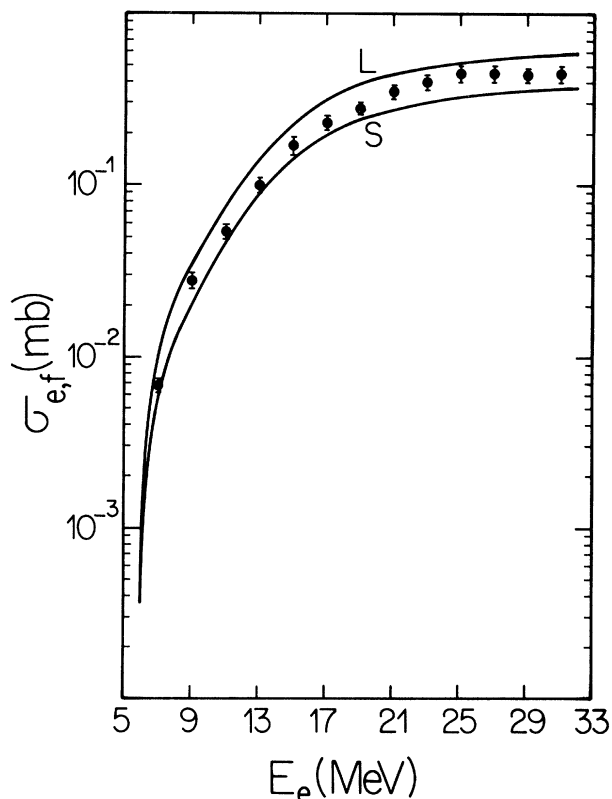


FIG. 3. Data points: electrofission cross section of ^{232}Th (Ref. 13). Curves: photofission cross sections from Saclay (S) and Livermore (L) integrated in the $E1$ virtual-photon spectrum.

sion cross sections with the $E1$ virtual-photon spectrum; as a result, if the photofission is a pure $E1$ process those curves correspond to a pure electrofission process too. On the other hand, if we assume an $E2$ component exhausting $\sim 70\%$ of the isoscalar energy-weighted sum rule, as in the electrofission of the ^{236}U ,⁹ the curves shown in Fig. 3 should underestimate the electrofission cross sections by $\sim 30\%$ between 20 and 30 MeV. Using Saclay's results (curve S in Fig. 3) in the data interpretation, we conclude that the $^{232}\text{Th}(e,f)$ process cannot be explained as proceeding only through pure $E1$ transitions. On the other hand, the Giessen electrofission cross section falls systematically below the Livermore $E1$ curve (curve L in Fig. 3); therefore no physical information can be outlined. It is possible to speculate about miscalculation of the $E1$ virtual-photon spectrum, as suggested recently;¹⁴ however, it is worth

remembering that the $E1$ virtual-photon spectrum calculation was tested experimentally *again* in a recent work carried out at the National Bureau of Standards.¹¹

As concluding remarks, we would like to say that our results suggest that the photofission cross section for ^{232}Th from Livermore is probably more reliable than the one obtained at Saclay. Therefore, by examining Fig. 3 it is clear that there is a need for further electrofission studies of ^{232}Th . We are performing very detailed measurements of the ^{232}Th electrofission cross section, in the energy range 5–32 MeV, which will be the subject of a forthcoming publication.

This work was supported in part by the Conselho Nacional de Desenvolvimento Científico e Tecnológico and by the Fundação de Amparo à Pesquisa do Estado de São Paulo.

¹J. D. T. Arruda-Neto and B. L. Berman, Nucl. Phys. A349, 483 (1980).

²J. D. T. Arruda-Neto *et al.*, Nucl. Phys. A389, 378 (1982).

³J. D. T. Arruda-Neto, J. Phys. G 10, 101 (1984).

⁴D. H. Dowell *et al.*, Phys. Rev. Lett. 49, 113 (1982).

⁵Lawrence Livermore National Laboratory Report No. UCRL-78482, edited by B. L. Berman, 1976.

⁶A. Veyssi re *et al.*, Nucl. Phys. A199, 45 (1973).

⁷J. T. Caldwell *et al.*, Phys. Rev. C 21, 1215 (1980).

⁸W. C. Barber, Phys. Rev. 111, 1642 (1958).

⁹J. D. T. Arruda-Neto *et al.*, Phys. Rev. C 22, 1996 (1980).

¹⁰H. A. Bethe and L. C. Maximon, Phys. Rev. 93, 768 (1954); H. Davies *et al.*, *ibid.* 93, 788 (1954).

¹¹W. R. Dodge *et al.*, Phys. Rev. C 28, 150 (1983), and references herein.

¹²J. E. Gindler *et al.*, Phys. Rev. 104, 425 (1956).

¹³J. Aschenbach *et al.*, Z. Phys. A 292, 285 (1979).

¹⁴H. Str her *et al.*, Phys. Rev. Lett. 47, 318 (1981).